# Application of mathematical search algorithms for unknown material properties in Additive Manufacturing simulations

Aaron Flood[1] and Frank Liou[1]

[1]Mechanical and Aerospace Engineering, 194 Toomey Hall, Rolla, 65409, MO, USA.

Contributing authors: ajfrk6@umsystem.edu; liou@umsystem.edu;

**Abstract**

## 1 Introduction

### 1.1 Additive manufacturing (AM) simulations

Additive manufacturing (AM) is an emerging manufacturing technique which has the potential to revolutionize manufacturing. In order to realize this revolution, it is necessary to be able to produce components reliably and to understand the process well enough to ensure that builds are consistent enough that the performance of the completed build can be guaranteed. In order to do this, researchers and manufacturers have turned to mathematical modeling in order to understand the process Wang and Chen (2021).

The differences in simulation techniques can vary based on the desired response from the simulation and the underlying assumptions which were made during the development of the models. One example of this can be seen when comparing the mathematical models presented in Moges et al (2020), Roy and Wodo (2020), and Moges et al (2020). They all attempt to model roughly the same aspect of the build but take very different approaches. Moges et al (2020) take purely physics based approach to the solution and works from first principal of the physical process being modeled. On the contrary, Roy and Wodo (2020) is a data driven model which used a breadth of data to develop a mathematical which properly predicts the material behavior. In between these

models exists Moges et al (2020) which attempts to marry the two approaches and develop a physics based model which uses data to improve accuracy. The one unifying characteristic of these, and all, mathematical models, is the need for the inclusion of a dataset which defines the behavior of material being investigated, this is colloquially referred to as the material properties. These material properties can vary in literature and this variance in values can lead to a discrepancy in simulation results Daryabeigi (2011).

Though variation exists in the literature, values can be found and used when the material is well characterized and published. An example of a well published material is Ti-64 Welsch et al (1993), Boivineau et al (2006), and Fan and Liou (2012). However, for materials which are not well understood and published, such as specific aluminum alloys Lundberg (1994) and Lundberg (1994), there is a need to determine the material properties, or at a minimum, develop the dataset which produces the most accurate simulation results. This can be accomplished by expending the necessary resources to measure the needed properties using advanced equipment. This process can be expensive and time-consuming which has led to the development of material simulations which attempt to predict the material properties. Though faster and cheaper than experimental results, they, like all simulations, have an error that is associated with them. Using these values alone can lead to unknown error stack up in the AM models. This problem also applies to materials where the tolerances for alloying elements is so wide that specimen of the same alloy can have different material properties.

In order to develop a dataset which produces accurate AM simulation results, a multi-objective optimization scheme can be used as a search algorithm to determine the dataset which produces the most realistic results. This can be used to develop a dataset for a new alloy along with for a specific piece of stock which has been procured from a supplier.

This work will aim to address one of the current desires in metal AM which is to be able to produce parts out of aluminum which is shown by the volume of effort being put into aluminum AM (Qi (2020), Weiss (2019b), Weiss (2019a)). The challenge associated with this stems from the wide range of alloys which have wildly varying material properties which are not well published. One of the weldable high strength alloys which has been targeted for metal AM is 7050 Singh (????). Though the material is widely available, temperature dependent material properties are not readily available. Therefore, this work will find material properties in literature which are an approximation of the 7050 aluminum, namely sister alloys with similar compositions, as a starting point for the search algorithm and determine a material dataset which produces more accurate AM simulation results.

## 1.2 Simulation description

The model used in this study was developed in house and is detailed in **??**. This simulation has the express goals of being efficient while still holding true

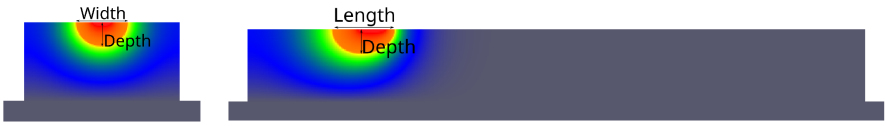


(a) Width (b) Length

**Fig. 1**: Example measurements of the melt pool

to physics models. In order to accomplish this, it heavily leverages GPU processing utilizing image processing techniques. The simulation was developed with laser directed energy deposition (DED) processes in mind, however, it was developed in a modular manner such that it can be applied to most metal AM processes.

The main objective of the model is to accurately predict the thermal history of the build. This was shown to be true in **??** where the model was able to predict the width of the melted track with approximately 3% error and the depth within 1.7 resolution steps (which was approximately 20% error).

# 2 Tuning algorithm implementation

## 2.1 Selection of Properties

In order to reduce the complexity of the search algorithm, a sensitivity analysis was performed in **??**. This work began by finding the material properties which were needed in the models these can be seen in Table 1.

**Table 1**: Key material properties in thermal modeling of AM

| Material Property | Reference |
|---|---|
| Solidus temperature | Joseph R. Davis (2001), Lundberg (1994), Ulbirch (2014), ASM (2022) |
| Liquidus temperature | Joseph R. Davis (2001), Lundberg (1994), Ulbirch (2014), ASM (2022) |
| Solid density | ASM (2022), AmesWeb (2022) |
| Fluid density | ASM (2022), Schmitz et al (2012), Leitner et al (2017) |
| Specific heat | Lundberg (1994), Leitner et al (2017) |
| Thermal conductivity | Lundberg (1994), Leitner et al (2017) |
| Absorptivity | Funck et al (2014), Boyden and Zhang (2006), El-Hameed et al (2017) |

These properties were varied according to a Placket-Burman design of experiment in order to determine the properties which, when changed, had a statically significant effect on the resulting melt pool width, depth, and volume, as measured in Figure 1. Analyzing these results with Pareto charts of the standardized effects of the variables and partial regression plots of the residuals it was determined that the variables in Table 2. This work only

**Table 2**: Critical material properties

| |
|---|
| Laser absorption at 880°C |
| Laser absorption at 922°C |
| Thermal conductivity at 922°C |
| Thermal conductivity at 1491°C |
| Specific heat at 733°C |

focused on the material properties and the laser diameter was included due to the difficulty associated with accurately measuring the diameter.

## 2.2 Tuning algorithm description

The search algorithm which was chosen was the Nelder-Mead search algorithm Nelder and Mead (1965). This method was selected because it is one of the most popular direct search methods for minimization of functions. The Nelder-Mead approach is a local optimization search which does not rely on knowledge of the gradient to select the next search. This is critical for the application to simulation results because the gradient is unknown and finding it would involve running a large quantity of simulations. With simulation times that can reach into days long, this is a critical consideration. Instead of knowing the actual function, it relies on n+1 vertices. This means that a smaller number of simulation runs are needed to perform the minimization Wang and Shoup (2011).

The flow chart in Figure 2 is the flow which is used to determine the next search point.

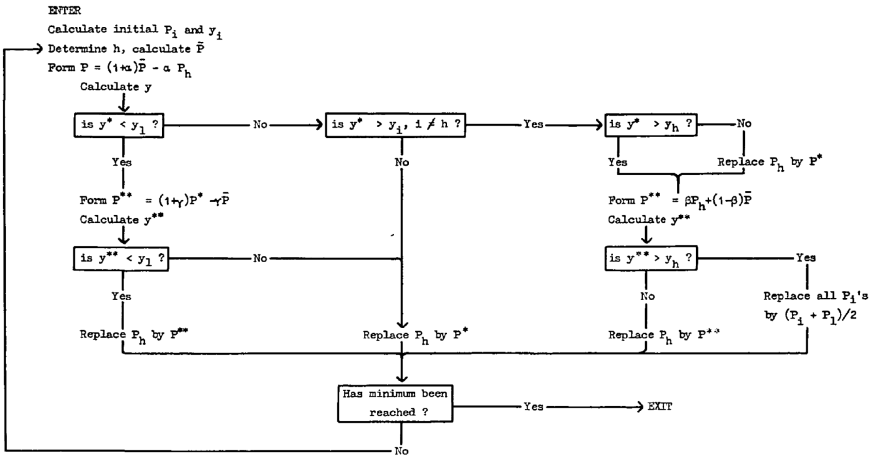


**Fig. 2**: Flow chart for the Nelder-Mead search algorithmNelder and Mead (1965)

In general, for each time step the reflection point is calculated using Equation 1 where $\alpha$ is the reflection coefficient.

$$P_{refl} = (1 + \alpha)P_{cent} - \alpha P_{high} \tag{1}$$

If this reflection point is smaller than the smallest current simplex value, then the expansion is calculated using Equation 2, where $\gamma$ is the expansion coefficient.

$$P_{exp} = \gamma P_{refl} - (1 - \gamma)P_{center} \tag{2}$$

If the expansion point is smaller than the reflection point then the expansion point is used to replace the largest simplex member. Otherwise, if the reflection point is larger than the expansion point the reflection point is used to replace the largest member of the simplex, and the algorithm is restarted.

If the reflection point is larger than the smallest simplex point and smaller than the second largest point then the highest point of the simplex is replaced with the reflection and the algorithm is restarted.

If the reflection point is between the simplex high and second highest value, a contraction is calculated, using Equation 1 with the highest values being replaced with the reflection, otherwise the contraction is calculated with the original simplex still using Equation 1, where $\beta$ is the contraction coefficient.

$$P_{cont} = \beta P_{high} - (1 - \beta)P_{cent} \tag{3}$$

If the contraction point is smaller than the largest point of the simplex the contraction replaces the largest point and the algorithm is continued. However if the contraction point is larger than the highest point, a shrink step is performed, detailed in Equation 4, where $\delta$ is the shrink coefficient, and the algorithm is restarted.

$$P_i = \delta P_i + (1 - \delta)P_{low} \tag{4}$$

## 2.3 Tuning and Simulation setup

For this study, the Nelder Mead search algorithm parameters which were used can be seen in Table 3. These parameters were chosen because they fell within

**Table 3**: Nelder-Mead algorithm parameters

| Parameter | Value |
|---|---|
| $\alpha$ | 5.0 |
| $\gamma$ | 10.0 |
| $\beta$ | 0.5 |
| $\sigma$ | 0.5 |

the guidelines from the algorithm description and after trial and error produced the most efficient tuning Nelder and Mead (1965).

The starting values which were used as the starting point for the search algorithm can be seen in Table 4. These values were chosen based on the values which were found in literature for similar aluminum alloys. The laser diameter which was chosen based on the measuring of a melt track width on a substrate.

**Table 4**: Material properties found in literature

| Property | Material Temp. | Value | Ref. |
|---|---|---|---|
| Laser absorption | 880°C | 15.0% | Boyden and Zhang (2006) |
| Laser absorption | 922°C | 30.0% | Boyden and Zhang (2006) |
| Thermal conductivity | 922°C | 88.8 $\frac{W}{mK}$ | Leitner et al (2017) |
| Thermal conductivity | 1491°C | 104.9 $\frac{W}{mK}$ | Leitner et al (2017) |
| Specific heat | 733°C | 1108.0 $\frac{J}{kgK}$ | Leitner et al (2017) |
| Laser diameter | | 1.6 mm | |

The experimental setup which was used was a simple laser scanning of the surface of a substrate, as shown in Figure 3, with the parameters shown in Table 5. This was chosen in order to simplify the experiment. This setup removes the complexity associated with adding material including the rate of material addition, molten metal flow parameters and acceleration effect associated with turning during deposits.

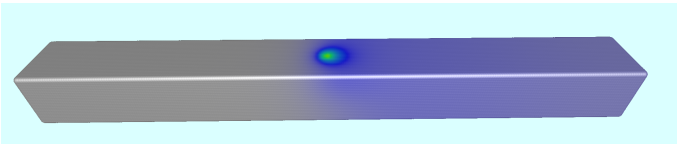

**Fig. 3**: Example of simulation setup used to determine melt track size

**Table 5**: Experimental constants used in tuning experiments

| Parameter | Value |
|---|---|
| Resolution | 100 $\mu m$ |
| Laser Power | 1,750 W |
| Laser Scan Speed | 1143 mm/min |
| Laser Profile | Top Hat |
| Scan Length | 77 mm |
| Substrate dimensions | 82 mm x 8 mm x 8 mm |

## 2.4 Simulation analysis

Upon completion of each simulation run, the saved data files were analyzed to determine the regions of the simulation which had melted. This was done by developing a map which marked the locations of the domain which had ever

been in the fluid phase. This map was then used to determine the width and depth of the melt track along the scan length, excluding the beginning and end where effects from starting and stopping motion would affect the results. These width and depth measurements along the scan length were averaged to develop a single measurement which could be compared to experimentation.

The experimental results were similarly developed, however instead of a continuous set of measurements, there were 4 discrete measurements. These were obtained by slicing the substrate at the prescribed locations using a Wire electrical discharge machine (EDM). These slices were polished and etched in order to make the microstructural differences visible, an example of this can be seen in Figure 4.

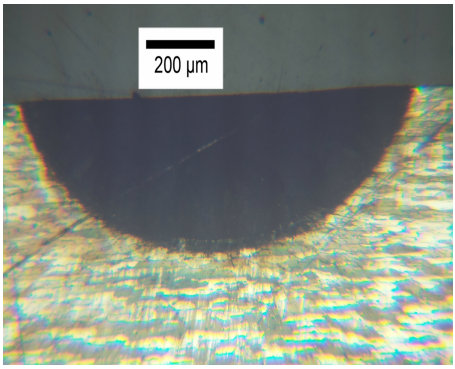


**Fig. 4**: Example of sliced, polished, and etched slice from experimentation

In order for the Nelder-Mead search to function properly, a response variable needed to be defined. This function needed to characterize the accuracy of the build into a single parameter which could be minimized and upon minimzation would result in the most accurate simulation. To accomplish this goal, Equation 5 was developed. This equation takes into account the error in the width of the simulation along with the error of the depth. If this equation results in a non-negative number where 0 represents a simulation which perfectly matched experimentation.

$$Response = \left( \frac{|Sim.\ Width - Exp.\ Width|}{Exp.\ Width} + \frac{|Sim.\ Depth - Exp.\ Depth|}{Exp.\ Depth} \right) * 100 \tag{5}$$

# 3 Results

## 3.1 Search algorithm results

The search algorithm was allowed to search the space to determine the best material properties. The resulting response variables can be found in Figure 5.

Where the blue markers indicate parameter sets which developed a melt track and the red one did not have the energy density to produce a melt track. Due

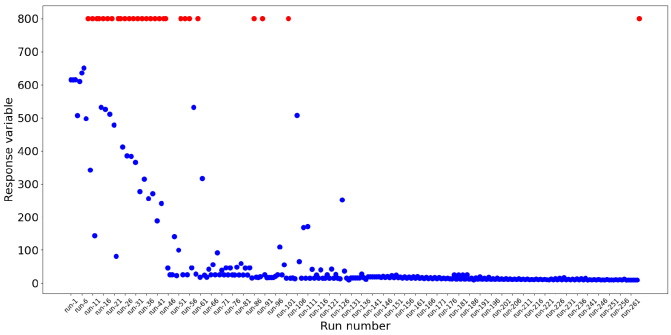


**Fig. 5**: Response variable of the search algorithm for material properties and laser diameter

to the vast difference in scales of the initial responses and the final response variables, a new plot was created which has a max Y value of just over 30. In this plot the blue plots are ones which have a response variable less than 30, the green markers are those which completed with a melt track but had response variables greater than 30, and the red markers are those which did not produce a melt track. In addition to these plots the error in the width

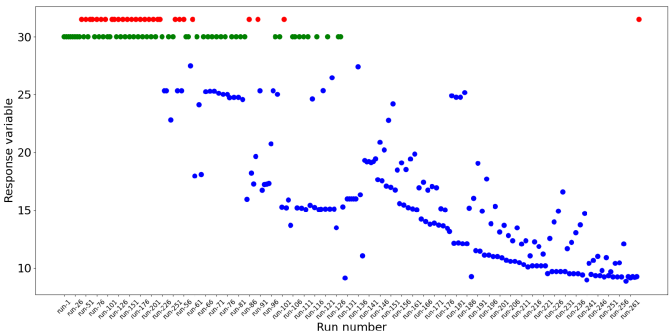


**Fig. 6**: Response variable of the search algorithm for material properties and laser diameter with max y axis value of 30

and depth were plotted and can be seen in Figure 7. In these plots, it can be seen that the error in the width is 8.83% and the error in the depth is 0.03%. It is not fully understood why all the error is coming from width, however it is theorized that this is a product of difference in the size of the width vs the depth since the width is nearly triple that of the depth.

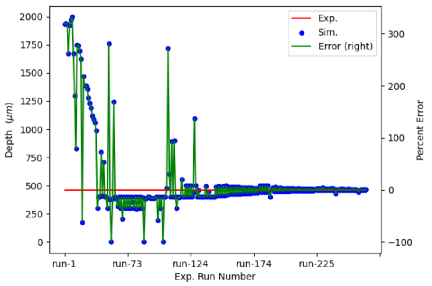


(a) Melt track depth

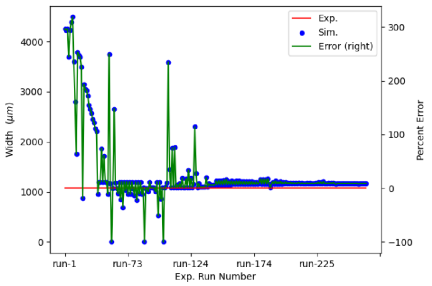


(b) Melt track width

**Fig. 7**: Error in the individual runs of the simulations during the tuning algorithm

The search algorithm completed and reduced the combined error from over 600% when starting from the material properties found in literature for a generic aluminum material properties, found in Table 4, to 9.1% when using the values found in Table 6

**Table 6**: Optimized material properties and laser diameter dataset for the developed simulation

| Property | Material Temp. | Value |
|---|---|---|
| Laser absorption | 880°C | 16.8% |
| Laser absorption | 922°C | 10.0% |
| Thermal conductivity | 922°C | 32.2 $\frac{W}{mK}$ |
| Thermal conductivity | 1491°C | 152.3 $\frac{W}{mK}$ |
| Specific heat | 733°C | 2957.6 $\frac{J}{kgK}$ |
| Laser diameter | | 0.864 mm |

### 3.2 Search results validation

In order to ensure that the tuning results were valid across laser travel speeds and power levels a range of 8 other parameters were compared, the values used can be seen in Table 7.

## 4 Conclusions

## References

AmesWeb (2022) ALUMINUM 6061 MATERIAL PROPERTIES. https://amesweb.info/Materials/Aluminum-6061-Properties.aspx

**Table 7**: Validation processing parameters

| Exp. Id. | Scan speed (mm/min) | Laser Power (W) |
|---|---|---|
| 1 | 762 | 1000 |
| 2 | 762 | 1500 |
| 3 | 762 | 1250 |
| 4 | 1143 | 1250 |
| 5 | 1143 | 1500 |
| 6 | 1524 | 1750 |
| 7 | 1524 | 1500 |
| 8 | 1524 | 2000 |

ASM (2022) Aluminum 6061-T6; 6061-T651. http://asm.matweb.com/search/SpecificMaterial.asp?bassnum=MA6061T6

Boivineau M, Cagran C, Doytier D, et al (2006) Thermophysical Properties of Solid and Liquid Ti-6Al-4V (TA6V) Alloy. International Journal of Thermophysics 27(2):507–529. https://doi.org/10.1007/PL00021868

Boyden SB, Zhang Y (2006) Temperature and Wavelength-Dependent Spectral Absorptivities of Metallic Materials in the Infrared. Journal of Thermophysics and Heat Transfer 20(1):9–15. https://doi.org/10.2514/1.15518

Daryabeigi K (2011) Thermal Properties for Accurate Thermal Modeling

El-Hameed AMA, Abdel-Aziz YA, El-Tokhy FS (2017) Anodic Coating Characteristics of Different Aluminum Alloys for Spacecraft Materials Applications. Materials Sciences and Applications 08(02):197–208. https://doi.org/10.4236/msa.2017.82013

Fan Z, Liou F (2012) Numerical Modeling of the Additive Manufacturing (AM) Processes of Titanium Alloy. In: Amin AN (ed) Titanium Alloys - Towards Achieving Enhanced Properties for Diversified Applications. InTech, https://doi.org/10.5772/34848

Funck K, Nett R, Ostendorf A (2014) Tailored Beam Shaping for Laser Spot Joining of Highly Conductive Thin Foils. Physics Procedia 56:750–758. https://doi.org/10.1016/j.phpro.2014.08.082

Joseph R. Davis (2001) Aluminum and Aluminum Alloys Davis.pdf. In: Alloying: Understanding the Basics. ASM International

Leitner M, Leitner T, Schmon A, et al (2017) Thermophysical Properties of Liquid Aluminum. Metallurgical and Materials Transactions A 48(6):3036–3045. https://doi.org/10.1007/s11661-017-4053-6

Lundberg S (1994) Material Aspects of Fire Design

Moges T, Yang Z, Jones K, et al (2020) HYBRID MODELING APPROACH FOR MELT POOL PREDICTION IN LASER POWDER BED FUSION ADDITIVE MANUFACTURING p 15

Nelder JA, Mead R (1965) A Simplex Method for Function Minimization. The Computer Journal 7(4):308–313. https://doi.org/10.1093/comjnl/7.4.308

Qi Y (2020) A high strength Al–Li alloy produced by laser powder bed fusion_ Densification, microstructure, and mechanical properties. Additive Manufacturing p 10

Roy M, Wodo O (2020) Data-driven modeling of thermal history in additive manufacturing. Additive Manufacturing 32:101,017. https://doi.org/10.1016/j.addma.2019.101017

Schmitz J, Hallstedt B, Brillo J, et al (2012) Density and thermal expansion of liquid Al–Si alloys. Journal of Materials Science 47(8):3706–3712. https://doi.org/10.1007/s10853-011-6219-8

Singh A (????) Additive Manufacturing Of Al 4047 And Al 7050 Alloys Using Direct Laser Metal Deposition Process p 140

Ulbirch (2014) 6000 & 7000 Series Aluminum Alloy

Wang D, Chen X (2021) Closed-Loop High-Fidelity Simulation Integrating Finite Element Modeling With Feedback Controls in Additive Manufacturing. Journal of Dynamic Systems, Measurement, and Control 143(2):021,006. https://doi.org/10.1115/1.4048364

Wang PC, Shoup TE (2011) Parameter sensitivity study of the Nelder–Mead Simplex Method. Advances in Engineering Software 42(7):529–533. https://doi.org/10.1016/j.advengsoft.2011.04.004

Weiss D (2019a) Developments in Aluminum-Scandium-Ceramic and Aluminum-Scandium-Cerium Alloys. In: Chesonis C (ed) Light Metals 2019. Springer International Publishing, Cham, p 1439–1443, https://doi.org/10.1007/978-3-030-05864-7_180

Weiss D (2019b) Improved High-Temperature Aluminum Alloys Containing Cerium. Journal of Materials Engineering and Performance 28(4):1903–1908. https://doi.org/10.1007/s11665-019-3884-2

Welsch G, Boyer R, Collings E (1993) Materials Properties Handbook: Titanium Alloys. ASM international